



**HAL**  
open science

## Experimental study on dynamic effects of $H^-$ and $D^-$ negative ions in an ECR-plasma source

M. Mitrou, P. Svarnas, S. Béchu

► **To cite this version:**

M. Mitrou, P. Svarnas, S. Béchu. Experimental study on dynamic effects of  $H^-$  and  $D^-$  negative ions in an ECR-plasma source. 19th International Conference on Ion Sources, Sep 2021, Online, Canada. pp.012006, 10.1088/1742-6596/2244/1/012006 . hal-03654984

**HAL Id: hal-03654984**

**<https://hal.science/hal-03654984>**

Submitted on 22 Nov 2022

**HAL** is a multi-disciplinary open access archive for the deposit and dissemination of scientific research documents, whether they are published or not. The documents may come from teaching and research institutions in France or abroad, or from public or private research centers.

L'archive ouverte pluridisciplinaire **HAL**, est destinée au dépôt et à la diffusion de documents scientifiques de niveau recherche, publiés ou non, émanant des établissements d'enseignement et de recherche français ou étrangers, des laboratoires publics ou privés.

PAPER • OPEN ACCESS

## Experimental study on dynamic effects of H and D negative ions in an ECR-plasma source

To cite this article: M Mitrou *et al* 2022 *J. Phys.: Conf. Ser.* **2244** 012006

View the [article online](#) for updates and enhancements.

You may also like

- [On the omnidirectional radiation via radially anisotropic zero-index metamaterials](#)  
Y. Yuan, N. Wang and J. H. Lim
- [Electronic structures of impurities and point defects in semiconductors](#)  
Yong Zhang and
- [Identifying the underlying physics of the ridge via 3-particle – correlations](#)  
Pawan Kumar Netrakanti and (for the STAR Collaboration)



The Electrochemical Society  
Advancing solid state & electrochemical science & technology

243rd ECS Meeting with SOFC-XVIII

**More than 50 symposia are available!**

Present your research and accelerate science

Boston, MA • May 28 – June 2, 2023

[Learn more and submit!](#)

# Experimental study on dynamic effects of $H^-$ and $D^-$ negative ions in an ECR-plasma source

M Mitrou<sup>1,2</sup>, P Svarnas<sup>1</sup> and S Béchu<sup>2</sup>

<sup>1</sup>High Voltage Laboratory, Electrical and Computer Engineering Department, University of Patras, Rion–Patras GR–26504, Greece

<sup>2</sup>Université Grenoble Alpes, CNRS, Grenoble INP (Institute of Engineering), LPSC-IN2P3, 38000 Grenoble, France

svarnas@ece.upatras.gr

**Abstract.** The electrostatic probe-based photo-detachment technique with one or two laser beams can provide insight on the negative ion absolute densities and dynamics, respectively, in electronegative plasmas. In this work, this diagnostic is installed in the ECR-driven (2.45 GHz) negative ion source “Prometheus I” and details of the setup design along with main underlying physics are discussed. Potential origins of signal distortions and thus erroneous employment of this technique are demonstrated. Based on these observations,  $H^-$  and  $D^-$  negative ion densities and temperatures are measured in a reliable manner. The experiments are carried out for variable microwave power (2.45 GHz), at 1.33 Pa, unveiling two distinct kinetic equilibriums of the negative ions, in both gases, and an isotope effect.

## 1. Introduction

Hydrogen negative ions ( $H^-$ ) are important in astrophysics, particle accelerators, and particularly nowadays in fusion science where they are being accelerated and then neutralized to form high energy atom beams for heating fusion plasmas [1]. However, in the latter case, and towards the international collaboration fusion project ITER, power level operation is being challenged with feeding deuterium to the ion sources. When the working gas of a negative ion source is changed from hydrogen to its isotope, deuterium, an “isotope effect” is observed; namely, several plasma characteristics such as the electron energy distribution, the atomic fraction, and the spectra of rovibrationally excited molecules change [2]. Inevitably, these changes affect the production and destruction processes of the  $D^-$  negative ions and hence their densities and energies. Thus, the application of diagnostic tools for probing and comparing directly properties related to  $H^-$  and  $D^-$  ions is mandatory.

Laser induced photo-detachment is a well-known and widely applied diagnostic technique for this purpose. In principle, a very modest laser pulse energy converts all the negative ions along the laser beam path into photo-detached electrons and atoms, which serve as “tags” of the negative ions from which they are originated [3]. The simplest technique for measuring the density of the tagged photo-detached electrons is the use of a Langmuir-type electrostatic probe, operated at the electron saturation part of its I-V curve. This concept has been broadly applied for many decades to measure the  $H^-$  and  $D^-$  negative ion densities.

On the other hand, quite surprisingly and at the same time challenging, a very limited number of works are devoted to the full exploitation of the photo-detachment technique, i.e., the determination of the negative ion energies-temperatures. This parameter is linked to the extracted negative ion beam quality and emittance, while it may be an appreciated input to numerical models of plasma kinetics in



ion sources. The fundamental physical concepts underlying this method when an electrostatic probe is used for the electron detection, implies [4]: (i) the creation of a controlled perturbation in the negative ion density, followed by (ii) the measurement of the recovery of the negative ion density  $n_t^-$  towards its initial value  $n_0^-$ , and (iii) fitting the measured results to a physical model of the density recovery process, in which the ion thermal drift velocity plays a central role. In practice, a first laser shot detaches all negative ions in the irradiated volume and a reference, photo-detachment signal is acquired. A second laser shot is triggered after a delay time  $\Delta t$  and it detaches all negative ions that have flown into the laser irradiated volume during  $\Delta t$ . Thus, the probe generates a second photo-detachment signal, which is superposed with the reference one and lags that by  $\Delta t$ . By increasing the delay  $\Delta t$ , the amplitude of this second signal approaches the amplitude of the reference signal, progressively, providing thus information on the negative ion density recovery at different points in time [3]. Namely, by subtracting the reference signal from the mixed signal for each  $\Delta t$ , the second signal is isolated, and its peak is measured. The ratio between the isolated and the reference signal amplitudes equals to  $n_t^-/n_0^-$ , where  $n_0^-$  is conventionally estimated from the peak of the reference probe signal. Thus,  $n_t^-$  is determined.

To the best of our knowledge, the most indicative reports on the application of this process are the Refs. [4-9], concerning filament-driven sources. More recently, Kado et al. [10] proposed a novel and simple method to measure thermal and flow velocities of negative ions by making use of the photo-detachment technique in a steady-state linear divertor/edge plasma simulator MAP (material and plasma)-II. They stated that, flow measurements, especially for ions, is important in the divertor/edge region of fusion devices since the flow and its shear influence the plasma turbulence and the friction force against impurity contaminations.

Despite the afore mentioned works, there is a substantial lack of data on the energies of  $H^-$  and  $D^-$  negative ions formed in electron cyclotron resonance (ECR) driven sources. The present work is devoted to this topic. Experimental results are reported and commented, along with enlightening tips for avoiding experimental uncertainties. Overall, two distinct kinetic equilibriums of these ions are found, in both gases, and higher ion energies are estimated in the case of  $D^-$ , under the assumption of a ballistic model.

## 2. Experimental setup

The negative ion source “Prometheus I” and the electrostatic probe system are described elsewhere [11]. Note that the source is driven by five elementary ECR modules with permanent magnets (875 G) and all measurements are realized at 65 mm downstream of the ECR-zone middle planes (**Fig. 1**).

As regards the two-laser photo-detachment setup, **Fig. 1** depicts the actual concept. The beams of two independent Nd:YAG lasers (Quantel Brilliant EaZy) are coaxially aligned by means of appropriate optical components (see caption of **Fig. 1**). A multichannel pulse/delay generator (Berkley Nucleonics Corp; Model 525), coupled with a custom-made opto-isolating and amplifying unit, is employed for the flash lamp and Q-switch synchronization of the two lasers with a 4-ns resolution. A pyroelectric energy meter (Ophir Photonics; PE25BF-DIF-C), equipped with a diffuser for concentrated beams, is used for the beam energy determination. A fast photodetector (Ophir Photonics; FPS-10) allows for the monitoring of the temporal behavior of the laser pulses and its signal triggers the probe acquisition. To avoid any potential errors that arise from the use of conventional capacitive decoupling circuits, a wideband current transformer (Pearson Electronics 6585) provides the impulses generated by the photo-detached electrons. All signals are recorded on a wideband digital oscilloscope (LeCroyWaveSurfer 104Xs-A) and averaged in-situ to increase signal-to-noise ratio (>200 averaged samples). No further signal processing (filtering – smoothing) is applied during or after the acquisition.

The working gas is either  $H_2$  (99.999%; AirLiquide) or  $D_2$  (99.8%; Linde). The pressure is maintained constant at 1.33 Pa, based on previous optimization studies on the ratio between the electron and the negative ion densities. The total microwave (2.45 GHz) power is varied up to 0.9 kW. Two sets of measurements are conducted, providing mean values and standard deviations.

Source wall conditioning requires special attention since notable variations in the plasma properties are observed when the two gases are interchanged. This effect is attributed to the gas retention. To ensure wall recovery, i.e., eliminate this issue and achieve stable and reproducible plasma properties, various

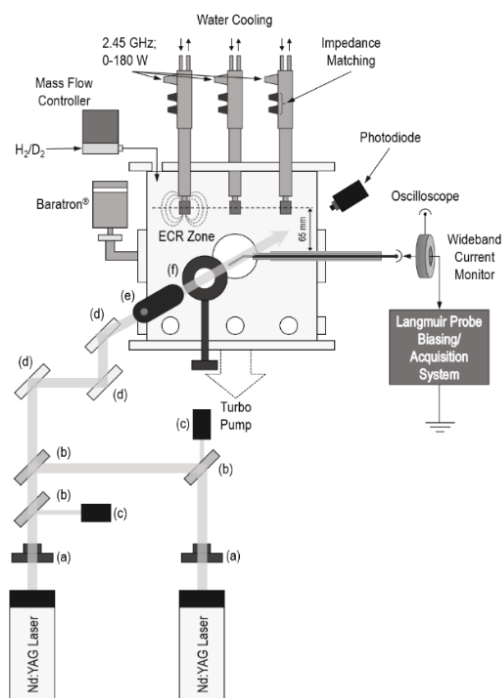


**Figure 1.** “Prometheus I” source and diagnostics. (a) Half wave plates on precision rotation mounts; (b) beam splitters; (c) laser beam dumps; (d) mirrors; (e) laser beam expander (8×), having Ø2.5 mm front and Ø5 mm rear diaphragms; (f) removable pyroelectric laser energy sensor.

trials led to the following protocol: each gas switch is followed by a bake-out of the source at 150°C, under base pressure ( $5.33 \times 10^{-5}$  Pa), for at least 30 h. Throughout the entire experimental series, the temperature of the source walls is not controlled in any manner, therefore it is solely influenced by the operating parameters and the sequence of the scheduled measurements. However, in between measurements, a 20-min interval is allowed for the thermal stabilization of the source.

### 3. Results and Discussion

It has been established that, for the proper design of the photo-detachment (either one- or two-laser version), four main parameters must be selected properly: (i) the laser wavelength with respect to the cross section of the photo-detachment reaction of the respective negative ions; (ii) the laser beam diameter with respect to the probe collection radius; (iii) the laser power density with respect to the saturation of the ratio between the density of the photo-detached electrons and the background negative ion density; and (iv) the probe bias with respect to the plasma potential. These points have been clarified previously [3]. Moreover, it is here underlined that the relative position (vertically; horizontally; rotationally) of the L-shaped probe tip with respect to the laser beam axis is a very sensitive parameter which may lead to highly distorted photo-detachment signals and, consequently, to erroneous data. **Figs. 2(a)-(c)** depict the problem by giving an indicative case. In a similar manner, even if the probe is “perfectly” aligned with the laser beam axis, different beam profiles (in terms of shape or energy distribution) result to modified signals. Thus, a beam expander and two diaphragms (**Fig. 1**) are employed to provide an almost homogeneous flux of 1064 nm photons, along a 5 mm in diameter cross section path. It was observed that the amplitude of the first distinct peak of the photo-detachment signal, which is used for the calculation of the steady state negative ion density,  $n_0^-$ , is quite immune to any reasonable misalignment or asymmetry. Nevertheless, these imperfections become crucial when ion dynamic effects are studied, since the probe tip must “see” two identical irradiative scenarios. **Fig. 2(d)** demonstrates the matched photo-detachment signals achieved from the two lasers, after following the above precautions. Both signals are checked periodically during the experiments.

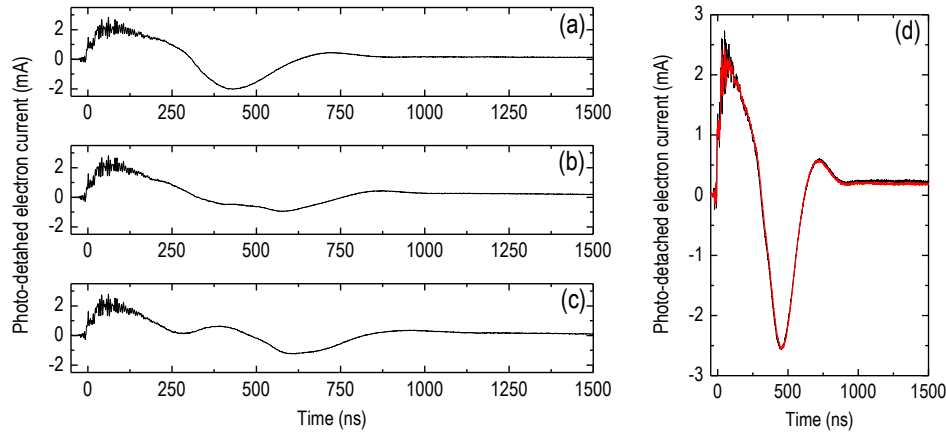


**Figure 2.** (a) Reference photo-detachment signal, when the probe tip and the laser beam are optimally aligned. Distorted signals due to vertical, lower displacement of the laser beam for about (b) 0.5 mm and (c) 1.1 mm, with respect to (a); horizontal and rotational alignments remain as in (a). (d) Matched signals induced by the two different laser beams, following the precautions discussed in the text; the red and the black curve are superposed. Operating conditions: H<sub>2</sub>; 600 W.

When the two lasers are triggered properly, mixed photo-detachment signals are recorded. **Fig. 3** (middle frames) provides corresponding examples for two delay times  $\Delta t$ ; 400 ns and 4  $\mu$ s. By sweeping  $\Delta t$  between 200 ns and 5  $\mu$ s, a bundle of such mixed signals is acquired. The subtraction of the reference signal (e.g., **Figs. 3(a1)** and **3(b1)**) from them, leads to the sought-out signals (e.g., **Figs. 3(a3)** and **3(b3)**). The amplitude of these signals is then divided by the amplitude of the reference signal and the recovery curves ( $n_e^- / n_0^-$  ratio vs. time) are constructed [3,4]. Two curve examples are given in **Fig. 4**.

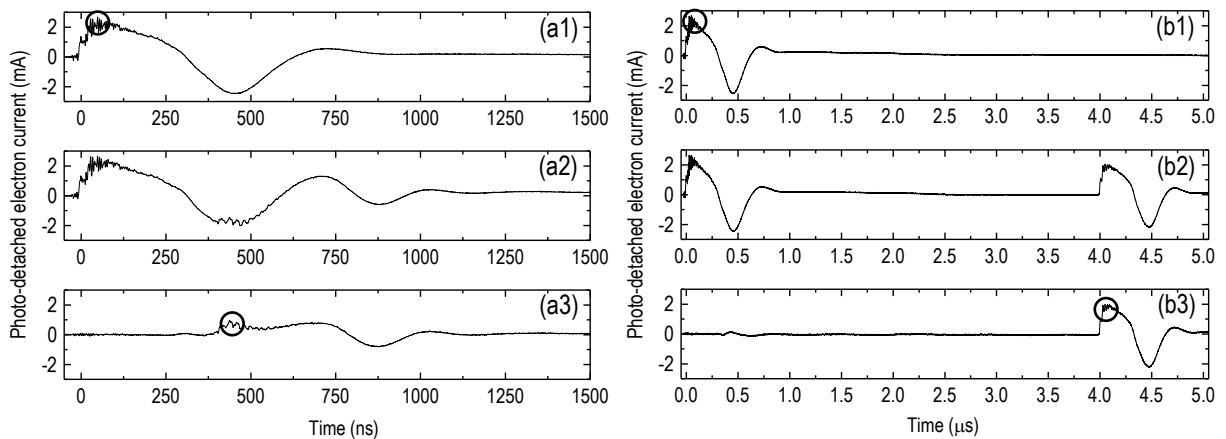


**Figure 3.** (a1) Single-laser photo-detachment signal. (a2) Double-laser photo-detachment signal, with  $\Delta t = 400$  ns. (a3) Subtraction signal, i.e., (a2 – a1). (b1) to (b3) Similar, with  $\Delta t = 4$   $\mu$ s. The inset circles define the amplitudes used for the calculation of the  $n_e^- / n_0^-$  ratio. Operating conditions: H<sub>2</sub>; 600 W.

It is here attempted to fit to the data a ballistic model [12], assuming two ionic populations of different temperatures [8]. Under the present conditions, the model traces acceptably the data up to about 2  $\mu$ s (**Fig. 4**). Fitting for longer recovery times, increases the overall least squares error significantly. According to this model, “cold” ions have energy less than 0.05 eV in both H<sub>2</sub> and D<sub>2</sub> plasmas, whereas “hot” ions achieve higher energies in D<sub>2</sub>. In any case, the “cold” negative ions dominate the “hot” ones, with a fraction of about 65–70% (**Fig. 4**). Besides, two electronic populations have been observed [11]. Indicative (900 W) plasma features, in H<sub>2</sub> | D<sub>2</sub>, are:  $V_p = 7.1$  | 8.4 V;  $n_e^{cold} = 2.3$  | 3.8 ( $\times 10^{10}$  cm<sup>-3</sup>);  $n_e^{hot} = 4.3$  | 4.4 ( $\times 10^8$  cm<sup>-3</sup>);  $kT_e^{cold} = 0.7$  | 1.0 eV;  $kT_e^{hot} = 14.6$  | 14.5 eV; and  $n_0^- = 3.9$  | 4.1 ( $\times 10^9$  cm<sup>-3</sup>).

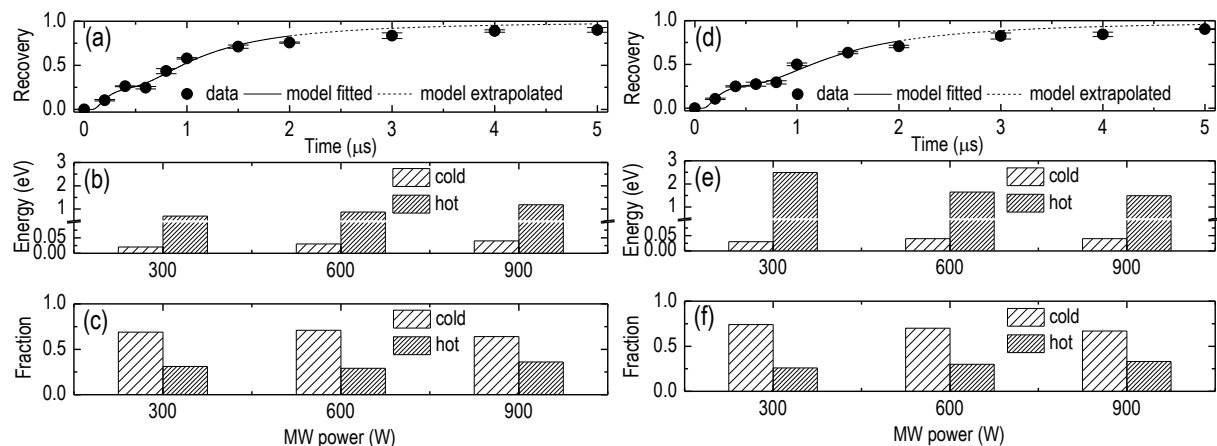


**Figure 4.** Ion density recovery (600 W): (a) H<sup>-</sup> and (d) D<sup>-</sup>. Ion energy versus MW power (be aware of the break on the vertical axis): (b) H<sup>-</sup> and (e) D<sup>-</sup>. Ion fraction versus MW power: (c) H<sup>-</sup> and (f) D<sup>-</sup>.

The production of two ionic populations and the elevated energy of the hot ions, should be traced back to their origin. In the ECR zones, inelastic collisions with hot electrons lead to vibrationally excited molecules which diffuse downstream, where the present measurements are realized. There, H<sup>-</sup> or D<sup>-</sup> ions are formed due to cold electron dissociative attachment (DA) on these molecules, which are expected to acquire only the energy of formation by DA, being thus cold. On the other hand, recombinative desorption processes on the metallic walls as a source of a wide spectrum of rovibrationally excited molecules, is broadly recognized. Ions formed near the walls, again by DA, are accelerated by the positive plasma potential difference, moving towards the bulk plasma, being thus hot(ter). This is in line with the constantly higher plasma potential measured in D<sub>2</sub> and the higher hot ion energy obtained, with respect to the H<sub>2</sub> case. Furthermore, we have measured increasing plasma potential versus the MW power, in both gases. Thus, higher power should lead to higher acceleration and finally increased energy for the hot ions. While this holds true in the H<sub>2</sub> case, the trend is different in the D<sub>2</sub> case. This implies that the accelerating ions are subject to various transport mechanisms in each gas–plasma, and it is another explicit difference with respect to the cold negative ions.

## Conclusions

The two-laser photo-detachment technique was applied in both H<sub>2</sub> and D<sub>2</sub> ECR plasmas. Two H<sup>-</sup> and D<sup>-</sup> ion populations were detected, i.e., a cold and a hot one, presumably due to different origins. Experimental data were treated under the assumption of a ballistic model which must be further assessed.

## Acknowledgments

This work was supported by the “Andreas Mentzelopoulos” Ph.D. Scholarships (M. Mitrou).

## References

- [1] Bacal M 2006 *Nucl. Fusion* **46** S250
- [2] Bacal M and Wada M 2020 *Plasma Sources Sci. Technol.* **29** 033001
- [3] Bacal M 2000 *Rev. Sci. Instrum.* **71** 3981
- [4] Bacal M 1993 *Plasma Sources Sci. Technol.* **2** 190
- [5] Devynck P, Auvray J, Bacal M, *et al.* 1989 *Rev. Sci. Instrum.* **60** 2873
- [6] Bacal M, Berlemont P, Bruneteau A M, *et al.* 1991 *J. Appl. Phys.* **70** 1212
- [7] Leroy R, Bacal M, Berlemont P, *et al.* 1992 *Rev. Sci. Instrum.* **63** 2686
- [8] Ivanov A A Jr 2004 *Rev. Sci. Instrum.* **75** 1754
- [9] Ivanov A A Jr, Bacal M, Rouillé C, *et al.* 2004 *Rev. Sci. Instrum.* **75** 1747
- [10] Kado S, Kajita S, Shikama T, *et al.* 2006 *Contrib. Plasma Phys.* **46** 367
- [11] Aleiferis S, Svarnas P, Béchu S, *et al.* 2018 *Plasma Sources Sci. Technol.* **27** 075015
- [12] Stern R A, Devynck P, Bacal M, *et al.* 1990 *Phys. Rev. A* **41** 3307